Suppression of pancreatic ductal adenocarcinoma growth by intratumoral delivery of attenuated *Salmonella typhimurium* using a dual fluorescent live tracking system

Sujin Zhou, Zhenggang Zhao, Yan Lin, Sijia Gong, Fanghong Li, Jinshun Pan, Xiaoxi Li, Zhuo Gao & Allan Z. Zhao

Published online: 20 May 2016.

Submit your article to this journal

Article views: 1071

View related articles

View Crossmark data

Citing articles: 3 View citing articles

Taylor & Francis
Taylor & Francis Group

RESEARCH PAPER

Suppression of pancreatic ductal adenocarcinoma growth by intratumoral delivery of attenuated *Salmonella typhimurium* using a dual fluorescent live tracking system

Sujin Zhou[a,*], Zhenggang Zhao[a,*], Yan Lin[a,*], Sijia Gong[a], Fanghong Li[a], Jinshun Pan[a], Xiaoxi Li[a], Zhuo Gao[b], and Allan Z. Zhao[a]

[a]Collaborative Innovation Center for Cancer Medicine, The Center of Metabolic Disease Research, Nanjing Medical University, Nanjing, Jiangsu Province, China; [b]Department of Clinical Laboratory, The Fourth Affiliated Hospital of Harbin Medical University, Harbin, Heilongjiang, China

ABSTRACT

Pancreatic ductal adenocarcinoma (PDAC) has the poorest prognosis among all malignancies and is resistant to almost all current therapies. Attenuated *Salmonella typhimurium* strain VNP20009 has been deployed as powerful anticancer agent in a variety of animal cancer models, and previous phase 1 clinical trials have proven its safety profiles. However, thus far, little is known about its effect on PDAC. Here, we established CFPAC-1 cell lines expressing an mKate2 protein and thus emitting far-red fluorescence in the subsequent xenograft implant. VNP20009 strain was further engineered to carry a luciferase cDNA, which catalyzes the light-emitting reaction to allow the observation of *salmonella* distribution and accumulation within tumor with live imaging. Using such VNP20009 strain and intratumoral delivery, we could reduce the growth of pancreatic cancer by inducing apoptosis and severe necrosis in a dosage dependent manner. Consistent with this finding, intratumoral delivery of VNP20009 also increase caspase-3 activity and the expression of Bax protein. In summary, we revealed that VNP20009 is a promising bacterial agent for the treatment of PDAC, and that we have established a dual fluorescent imaging system as a valuable tool for noninvasive live imaging of solid tumor and engineered bacterial drug.

Introduction

Pancreatic ductal adenocarcinoma (PDAC) is one of the most lethal human malignancies with a 5-year survival rate of less than 5%.[1] The poor prognosis of PDAC is mainly due to the early onset of local invasion, distant metastasis, and poor response to all available drugs. Due to the complex PDAC tumor microenvironment (abundant tumor stromal content [2] and hypoxia [3]), current clinical therapies invariably fail to deter this aggressive tumor. PDAC microenvironment supports tumor growth, promotes metastasis, and simultaneously serves as a physical barrier to drug delivery. However, because of these characteristics, the microenvironment of PDAC is an attractive target for bacteria.

Many bacterial genera, such as different variants of *Salmonella*,[4] *Clostridium* [5] and *Streptococcus pyogenes*,[6] have been shown to have successful suppressive effects on multiple animal tumor models, the most notable of which is pancreatic cancer.[7] Already, *Salmonella typhimurium* A1-R, a nutrient-deficient mutant,[8,9] and *Streptococcus pyogenes*[6] have been reported to significantly control xenograft pancreatic tumor growth. We focused on *Salmonella typhimurium* VNP20009, a genetically engineered attenuated strain that has a major advantage in producing no endotoxin through successful deletion of the *msbB* and *purI* genes.[10] This strain is also known to specifically target a variety of xenogenic cancer models.[11-14] Importantly, 2 phase

1 clinical trials have already proven its well-tolerated safety profiles.[15,16] However, its application in the treatment of pancreatic cancer remains to be explored.

To test the efficacy of VNP20009 in treating pancreatic tumor, we also developed a novel far-red fluorescent xenogenic pancreatic tumor model in animals. Such model will help us track the therapeutic effects on the tumor using living imaging. Biological tissues are transparent in 700–900 nm windows. The mKate2 is a monomeric far-red fluorescent protein whose excitation and emission spectra peak at 588 and 633 nm respectively, [17] making this protein a convenient tool for *in vivo* fluorescent imaging of targeted tissues. Therefore, we developed mKate2-expressing CFPAC-1 cell line, a well-established human pancreatic cell line, and deployed it in the subsequent xenograft model to test the efficacy of VNP20009 in the treatment of PDAC.

Results

Generation and characterization of fluorescent VNP20009 and pancreatic cell lines

We developed a system that allows us to simultaneously image both the implanted tumor and the treatment drug. VNP20009 was engineered to express luciferase for tracking the microbe in real time *in vivo*. CFPAC-1 cell lines carry a cDNA encoding

the mKate-2 protein emitting far-red fluorescence were used in subsequent xenografts for monitoring tumor growth and regression in animals. It has been reported that the expression of mKate-2 and luciferase have no effect on the biological behavior of parental cell.[18,19] Bioluminescence imaging (BLI) analysis confirmed that the light intensity, released from the VNP20009 strain expressing luciferase ("VNP20009-luc"), was proportional to bacterial counts ($r^2 = 0.99$). Additionally, VNP20009-luc displayed 0.36 ± 0.035 flux units per cfu *in vitro* (Fig. 1A, 1B).

To establish a CFPAC-1 pancreatic subcutaneous xenograft model with far-red fluorescence, the mKate2-expressing CFPAC-1 pancreatic cell lines were initially tested *in vitro*. The correlation between fluorescent signal and the cell numbers was assessed by visualizing the plated cells in cultured plates with an IVIS Spectrum Imaging System (Fig. 2A). The signal emitted was linear in relation to the cell numbers ($r^2 = 0.97$), indicating that there was a linear correlation between cell numbers and fluorescence intensity *in vitro* (Fig. 2B), which would help us semi-quantitatively evaluate the number of fluorescence-emitting cells in a tumor. We then performed an assay using a cell counting kit-8 (CCK8) to evaluate the response of the parental CFPAC-1 cells and the mKate2-expressing CFPAC-1 cells to the treatment with either VNP20009 or VNP20009-luc. Although significant inhibitory effects on cell proliferation were evident for either type of bacteria *in vitro* (P < 0.001, Fig. 2C), no significant difference was observed between VNP20009 and VNP20009-luc in their ability to suppress cell growth, suggesting that the expression of luciferase did not influence the effect of VNP20009. We also measured the growth rate of subcutaneous tumors of the parental CFPAC-1 and mKate2-expressing cells *in vivo* (Fig. 2D). The result indicated that the expression of mKate2 did not cause significant changes on the growth of CFPAC-1 implant *in vivo*.

For validation of the potential usage of mKate2-expressing CFPAC-1 pancreatic cell in tracking tumor growth *in vivo*, the cells were then implanted subcutaneously in the immune deficient nude mice, and the animals were imaged on day 15, 25 and 33 post implantation. Live imaging of the mice bearing mKate2 CFPAC-1 tumors showed the increase of signal intensity with tumor progression. However, most likely due to insufficient angiogenesis, central tumor necrosis was detected after 3–4 weeks (Fig. 2E). Accordingly, Tumor cell death was reflected by a decrease in signal intensity but not by size (Fig. 2F). Thus, CFPAC-1-mKate2 cells could be used as an effective model for detection of subcutaneous tumor development by noninvasively imaging.

VNP20009 inhibits the growth of pancreatic xenografts in vivo

The two tracking system was used to evaluate the anti-tumor potential of VNP20009 *in vivo*. Mice bearing pancreatic xenografts (approximately 60-100 mm^3) were assigned to one of 2 groups for different treatments: PBS or VNP20009-luc. The treatments were administered through a single intra-tumoral injection with VNP20009-luc at different doses (2×10^4 cfu/mouse or 2×10^6 cfu/mouse). Mice received different doses of VNP20009-luc did not exhibit any significant changes in body weight or any adverse behavioral effects relative to the PBS treated group (data not shown), but with a dose-dependent decrease in tumor size. At the end of the study, tumor growth was significantly inhibited by 27.3% in the group receiving VNP20009-luc 2×10^4 cfu/mouse (P < 0.02, Fig. 3A, 3B), and by 39.9% in the group receiving a higher dose of 2×10^6 cfu/mouse (P < 0.01; Fig. 3D, 3E). At the end of observation, the average tumor weight was 0.27g, or 0.2 g in the mice treated with 2×10^4 cfu/mouse or 2×10^6 cfu/mouse VNP20009-luc, respectively, compared to 0.42 g in mice injected with PBS alone (Fig. 3C, 3F). In a parallel control, a group of mice received a single intratumoral injection of 2×10^6 cfu/mouse of VNP20009. Consistent with the observations in cultured cells, no significant difference was observed on the anti-tumor effects between the parental strain VNP20009 and the VNP20009-luc (Fig. 3D, 3E, 3F). We further evaluated the efficacy of repeated injection of VNP20009-luc. Treatments were administered through 2 intra-tumoral injections of 2×10^6 cfu/mouse with the first injection delivered when tumor volume reached 60-100 mm^3 and the second injection 6 d later. The treated mice appeared normal and no obvious weight loss was observed during the treatment (data not shown). By day 19 of such
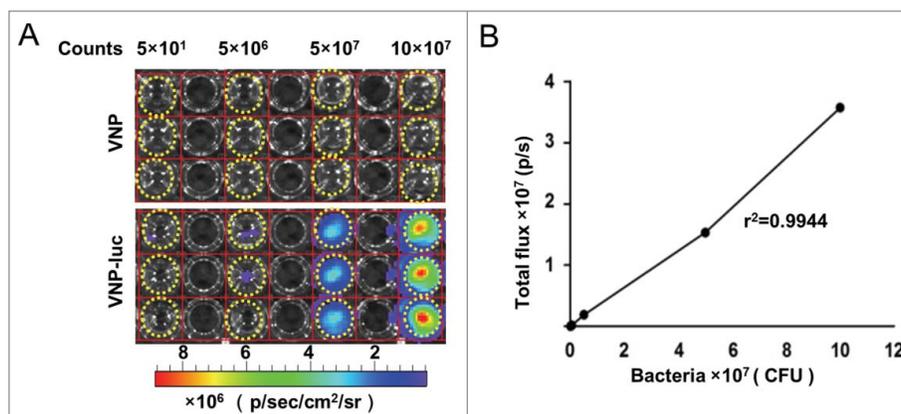
Figure 1. Characterization of VNP20009-luc *in vitro*. (A) VNP20009-luc cells were diluted to obtain numbers ranging from 50 to 1×10^8 cells, plated in duplicate wells, and imaged with IVIS Spectrum Imaging System. Wells containing VNP20009 served as controls. Dotted circles indicated the wells with bacteria. (B) Correlation between VNP20009-luc counts and bioluminescence ($r^2 = 0.99$). VNP and VNP-luc are abbreviations for VNP20009 and VNP20009-luc.

Figure 2. Characterization of mKate2-expressing CFPAC-1 cells *in vitro and in vivo*. (A, B) The mKate2-expressing CFPAC-1 cells were plated at different densities (500–5,000 cells) in 96-well plates, an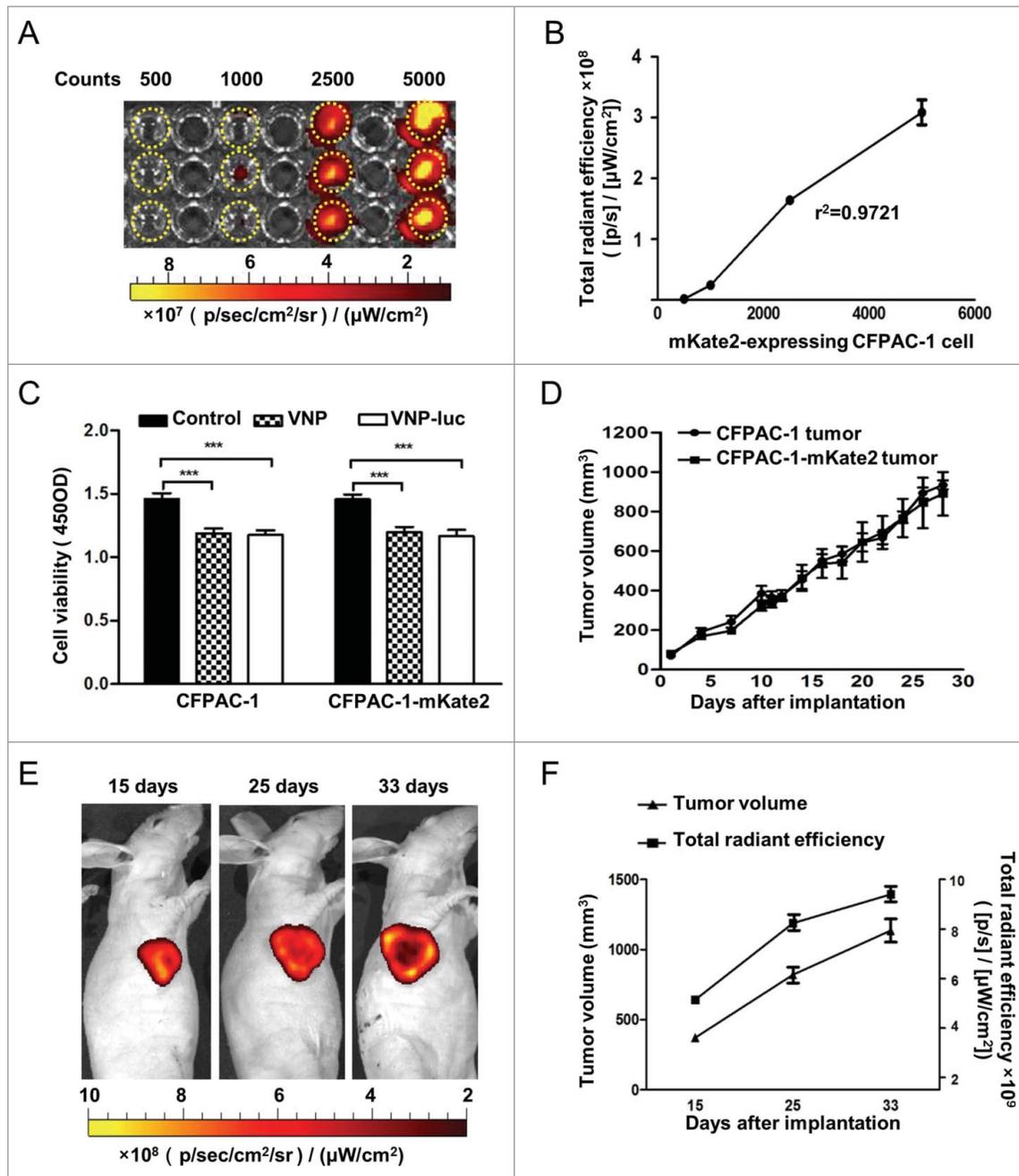d fluorescence signals were measured with IVIS Spectrum Imaging System ($r^2 = 0.97$), dotted circles indicated the wells with CFPAC-1-mKate-2 cells. (C) Cell viability was analyzed by CCK8 assay after the CFPAC-1 and CFPAC-1-mKate2 cells were co-cultured with VNP20009 or VNP200009-luc for 48 h, [***]$P < 0.001$. (D) The growth rate of subcutaneous tumors of the parental CFPAC-1 and mKate2-expressing cells were measured. Bars, mean $\pm$ SEM. (E) The mKate2-expressing CFPAC-1 cells were implanted in nude mice and the mKate2 fluorescent signal was measured on day 15, 25 and 33 after injection. Representative images are shown. (F) The tumor volumes and the corresponding total radiant efficiency were measured. Bars, mean $\pm$ SEM. VNP and VNP-luc are abbreviations for VNP20009 and VNP20009-luc.

treatment module, VNP20009-luc had significantly inhibited tumor volume growth by 66.2% ($P < 0.0001$), and the average tumor weights in the treated and the untreated group were 0.15 g and 0.47 g, respectively ($P < 0.0001$, Fig. 3G, 3H, 3I). On day 12 post the injection of 2×10^6 cfu/mouse, the expression of the luciferase gene of VNP20009 and far-red fluorescent protein mKate-2 of CFPAC-1 tumor cells were monitored using IVIS Spectrum Imaging System. All the tumors in PBS group displayed strong far-red fluorescence (Fig. 4A). The far-red fluorescent signal obtained from the

tumors had a lower intensity in the treated group compared to the PBS group, which was consistent with the perspective volumes of tumor. No far-red fluorescence was detected in the tumor center of the treated group, indicative of extensive central necrosis (Fig. 4A). Quantification of the signal emitted from tumors showed that a significant treatment-induced reduction in fluorescence signal intensity (Fig. 4B). Taken together, these results suggest that VNP20009 can significantly reduce the growth of CFPAC-1 pancreatic xenograft.
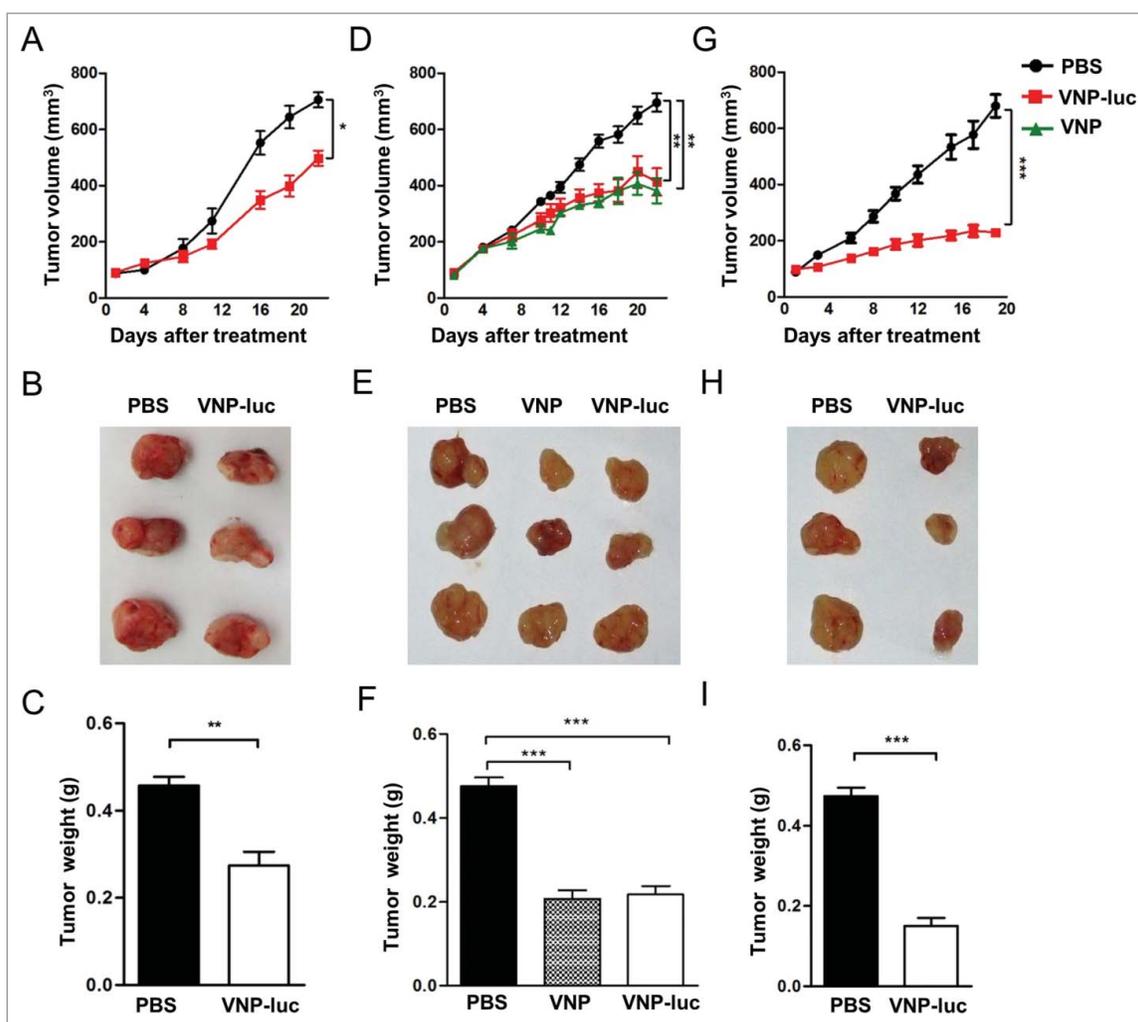
Figure 3. Therapeutic efficacy of VNP20009 against CFPAC-1 xenograft *in vivo*. (A to C) Mice bearing human pancreatic cancer CFPAC-1 xenograft received a single intra-tumoral injection of vehicle (PBS) or VNP20009-luc (2 × 10⁴ CFU/mouse, n = 10). (D to F) Mice received a single intratumoral injection of PBS, VNP20009 or VNP20009-luc (2 × 10⁶ cfu/mouse, n = 10). (G to I) Mice received 2 intra-tumoral injections of 2 × 10⁶ cfu/mouse with the first injection delivered when tumor volume reached 60–100 mm³ and the second injection 6 d later (n = 10). (C, F, and I) At the end of the treatment period, tumor tissues were dissected and weighed. *P < 0.05, **P < 0.01, ***P < 0.001. Bars, mean ± SEM. VNP and VNP-luc are abbreviations for VNP20009 and VNP20009-luc.

Tracking of VNP20009 distribution in vivo

We also verified the intensity and distribution of VNP20009 via live animal imaging. The strongest bacterial bioluminescent signal was mainly observed at the implanted tumor site, near tumor necrotic regions, and peripheral proliferative region of the tumor (Fig. 4A, 4B). Low bioluminescence was detected in areas from the abdomen and neck of the infected animals, which has been reported in some previous studies that VNP20009 can grow within lymph nodes, liver and spleen.[20] The sharply higher signals in tumor tissues than those non-tumor tissues indicated that VNP20009-luc preferred to accumulate within tumors. Both VNP20009-luc and VNP20009 preferentially accumulated and replicated in the tumors at a ratio of 366:1 to 3500:1 relative to the non-cancerous tissues with virtually identical bio-distribution profiles for either strain of bacteria, suggesting again that addition of luciferase in VNP20009 did not compromise its tumor targeting efficiency. Moreover, bacterial replication in tumors was also verified by bacterial culture of the ground tumor and non-tumor tissues (Fig. 4C). The tumors contained approximately 5.5 × 10⁶ cfu/g

of VNP20009-luc, corresponding to 0.16±0.055 flux units per cfu. The bioluminescence intensity of VNP20009-luc in tumors was lower than that *in vitro*, probably because the strain was in direct contact with the substrate luciferin *in vitro*, while the ability of luciferin to access the VNP20009-luc can be influenced by blood vessel structure and microenvironment within tumors.[21] Consistently, we observed extensive central necrosis in the tumors from the treatment group by histological analyses (Fig. 4D). These findings suggest that VNP20009 was capable of accumulating and inducing necrosis within pancreatic tumors.

VNP20009 promoted tumor apoptosis

To further understand VNP20009-induced tumor growth inhibition, we carried out immunohistochemical staining to initially follow the proliferation marker, Ki-67, in the tumor tissues. There were significantly fewer Ki-67-positive nuclei in the tumors of the treated mice than in those of the control mice (Fig. 5A, 5B). Further analysis of apoptosis markers showed an increase in caspase-3 activity and Bax protein expression
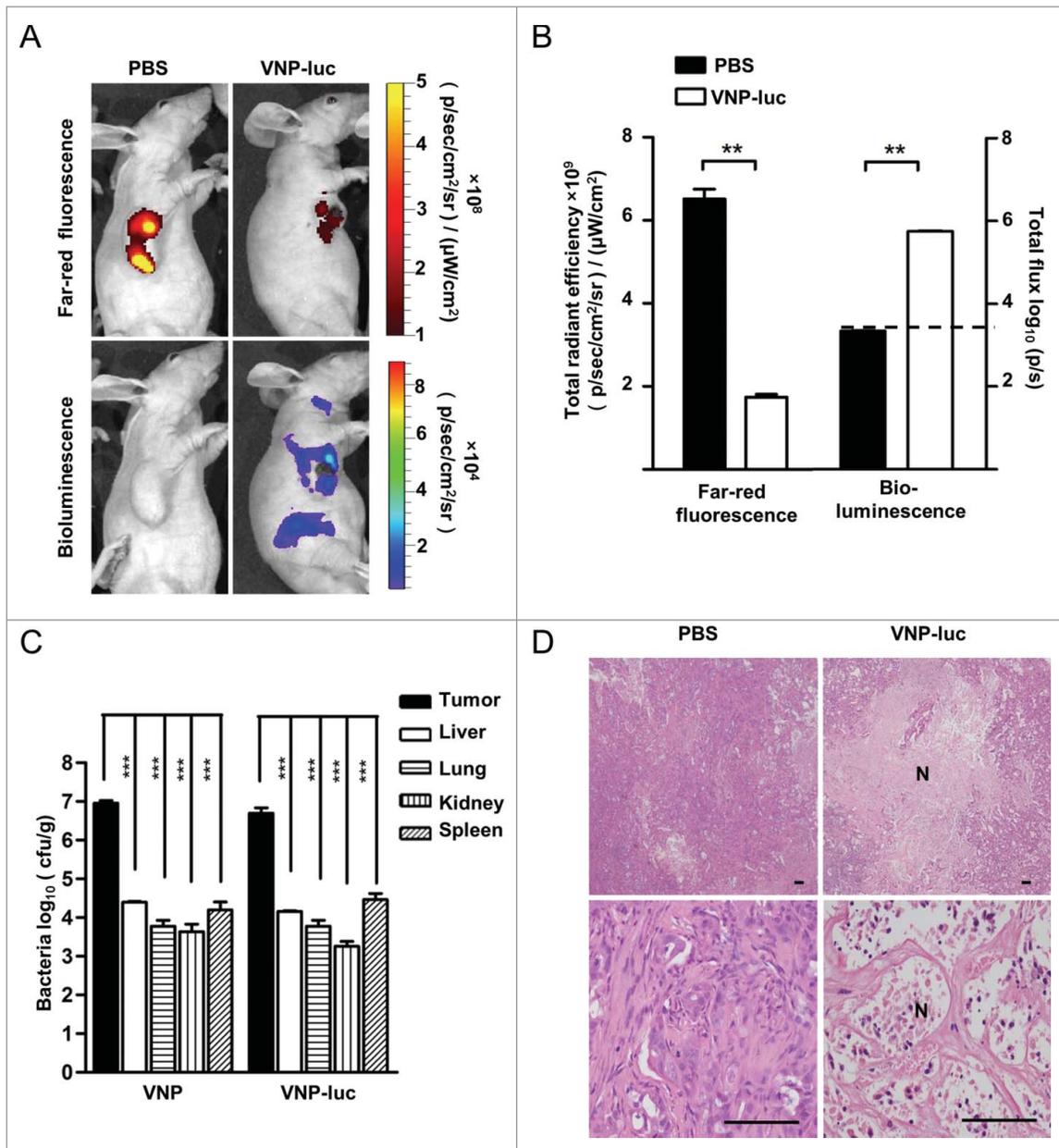
Figure 4. VNP20009 accumulated in CFPAC-1 tumors and caused tumor necrosis. (A) Bioluminescence from VNP20009-luc and far-red fluorescence from tumor cells were visualized with IVIS Spectrum Imaging System on day 12 post a single intratumoral delivery of 2×10^6 CFU/mouse of VNP20009-luc or PBS. Representative mice are shown. Tumor fluorescence = red, bacterial luminescence = rainbow. (B) Quantification of the far-red fluorescence and bacterial bioluminescent signal at tumor site, dash line indicated baseline nonspecific bioluminescent signal (n = 5). (C) Bacterial titer of VNP20009 or VNP20009-luc in tumors, livers, lungs, kidneys and spleens on day 12 post treatment (n = 5), [***]$P < 0.0001$ versus tumor, one-way analysis of variance test followed by Dunnett post hoc. (D). H&E staining of xenograft CFPAC-1 pancreatic tumor on the final day of a single intratumoral injection of 2×10^6 cfu of VNP20009-luc and PBS. Scale bars, 100 μm. N: necrosis, [**]$P < 0.01$, [***]$P < 0.001$. Bars, mean $\pm$ SEM. VNP and VNP-luc are abbreviations for VNP20009 and VNP20009-luc.

(Fig. 5C, 5D, 5E), indicating VNP20009 induced programmed cell death of CFPAC-1 pancreatic cancer *in vivo*. Taken together, these data support the notion that direct delivery of attenuated *Salmonella* strain, VNP20009, is an effective agent for killing pancreatic tumor.

Discussion

Although some bacterial therapies have shown treatment effect on pancreatic cancer in animal models,[6,9] no published studies thus far have used VNP20009 as the treatment agent of pancreatic cancer. To our knowledge, this is the first study to show

that VNP20009 alone, in a mere single or double intratumoral injection can cause significant regression of pancreatic carcinoma *in vivo*. The biggest advantage of VNP20009 as a pancreatic tumor treatment agent is its proven preclinical and clinical safety profiles or even efficacy result. Accordingly, repeated intravenous administration of VNP20009 in pet dogs with multiple spontaneous tumors led to tumor colonization and a complete elimination of tumor was seen in 4 of the 35 animals.[11] Two phase-1 clinical trials reported clinical tolerance following intravenous infusions of VNP20009 strains to metastatic melanoma patients, and at the highest tolerated dose, some tumor colonization was observed.[15,16]
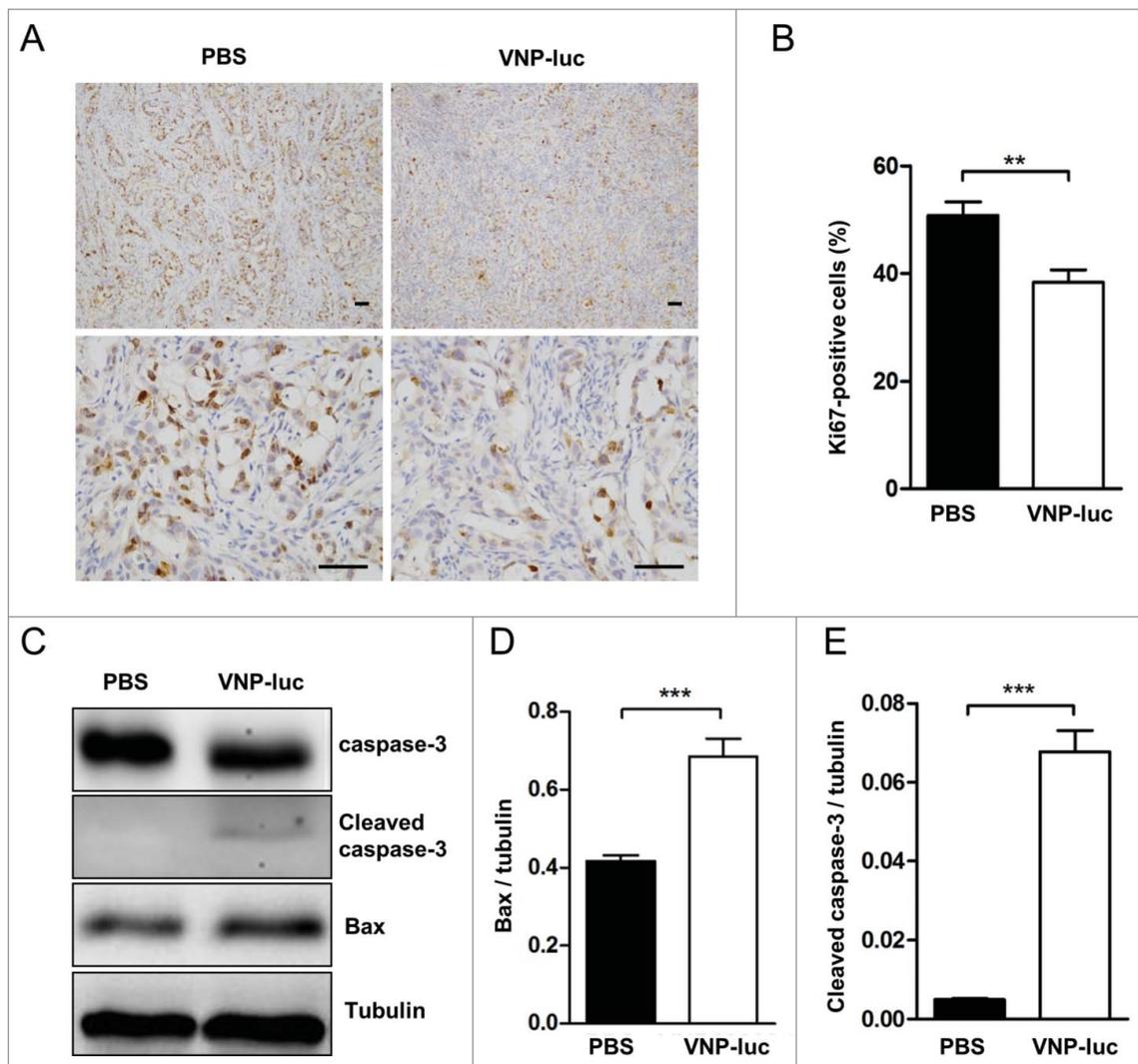
Figure 5. VNP20009 inhibited tumor growth and induced tumor apoptosis *in vivo*. (A) Representative immunohistochemical microphotographs of Ki67-stained xenograft CFPAC-1 pancreatic tumor sections. Proliferative nuclei were stained brown by Ki67. Scale bars, 50 μm. (B) Quantified data were determined by the number of Ki67-positive cells dividing the total number of cells in 5 randomly selected fields under light microscopy. (C) Western bolt analyses of Bax and caspase-3 in the tumors at the end of treatment of a single intratumoral injection of 2×10^6 cfu of VNP20009-luc or PBS. The expression of (D) Bax and (E) Cleaved caspase-3 were quantified and compared. n = 5 mice per group. **P < 0.01, ***P < 0.001. Bars, mean ± SEM. VNP-luc is abbreviation for VNP20009-luc.

In this study, we have created a double-fluorescent system that allowed us to concomitantly follow xenogenic tumor growth and metastatic status and microbe drug distribution in live animals. The mKate2 is a protein capable of emitting far-red fluorescence almost 3-fold brighter than that from mKate and 10-fold brighter than that of mPlum. Such high intensive far-red emission system also has the characteristics of excellent pH resistance, photo-stability, and low toxicity that make mKate2 a superior fluorescent tag for living imaging.[22] Bacteria as a tumor target agent can also be tracked in real time *in vivo* by imaging.[23] Thus, simultaneous live imaging of tumor cells and luciferase-bearing VNP20009 became possible with this double fluorescent model. The far-red fluorescent signal obtained from the tumor of VNP20009-treated group was lower than that from the PBS-treated group, which was in sharp contrast with the intense bioluminescence signal emitted from colonized VNP20009-luc within tumors. The fluorescent model can be further developed for non-invasively monitoring the formation of regional and distant metastases.

Pilot clinical trial of genetically modified VNP20009 has shown that intratumoral administration could cause bacterial colonization in malignant tissue for at least 15 d with no significant adverse effects in late stage refractory esophagus adenocarcinoma patients.[24] Therefore, we focused on intratumoral injection. A notable observation of our findings was the significant tumor suppressive effects in the CFPAC-1 pancreatic xenografts after a single intratumoral injection of VNP20009 (2×10^4 cfu/mouse). The dosage applied, 2×10^4 CFU/mouse was considerably below commonly used dosages in other studies.[12,25] In preclinical studies, VNP20009 has been used as a single-agent therapy at doses of over 1×10^6 cfu/mouse, or as a part of combinatorial therapy at doses well over the one applied in our studies.[26] Hoffman and colleagues have used *Salmonella typhimurium* A1-R to target and managed to suppress many types of tumor,[27,28] including pancreatic cancer.[8,29] To achieve treatment efficacy on pancreatic cancer, a high dose of *Salmonella typhimurium* A1-R, 1.5×10^8 CFU/mouse, was delivered intraperitoneally. The clinical safety profiles have not yet been

established. Thus, intratumoral delivery of low dose of VNP20009 may represent an excellent modality in bacterial treatment of pancreatic cancer.

The antitumor mechanisms of VNP20009 remain to be systematically defined. VNP20009 preferentially accumulated in xenogenic tumors at ratios of 366:1 to 3500:1 compared with the non-cancerous tissues and induced tumor necrosis and apoptosis through activating caspase and bax expression. Previous studies have shown that hypoxia condition develops rapidly within PDAC tumor.[30,31] *Salmonella* bacterium is known to preferentially replicate within the hypoxic areas of tumor, therefore promoting oncolysis and tumor necrosis.[32] Although a previous study found that a particular nutrient-dependent strain of *Salmonella* A1-R and *Streptococcus pyogenes* could activate the immune system to damage tumor cells,[6,33] other studies have shown that the anti-tumor effects of VNP20009 did not depend on the presence of T and B cells,[13] which is consistent with our findings here in immune-deficient nude mice.

In summary, we have successfully created a far-red fluorescence model of human pancreatic ductal adenocarcinoma and applied the system in the study of VNP20009 on pancreatic cancer. Our findings demonstrated that intra-tumoral delivery of VNP20009 alone, even by a single or double injection, can inhibit the proliferation of CFPAC-1 pancreatic xenografts and can induce apoptosis, thus offering the possibility that this clinically proven safe bacterial strain can be applied clinically for the treatment of pancreatic ductal adenocarcinoma.

Materials and methods

Animals

6- to 7-week-old athymic nude mice (Balb/c *nu/nu*) were obtained from Charles River, Beijing. The mice were allowed to adapt for 7 d before being subjected to experimental use. All experimental protocols were approved by the Research Ethics Committee of the Nanjing Medical University. All experiments were conducted in compliance with the guidelines for the care and use of laboratory animals and approved by Institutional Animal Care and Use Committee of Nanjing Medical University.

Cell culture

293FT cell lines and the pancreatic cancer CFPAC-1 were obtained from American Type Culture Collection (ATCC) and cultured under recommended conditions. The CFPAC-1 cell line was established from fragments of pancreatic (primary) and liver (metastatic) tumors.[34] In order to establish cell lines stably expressing far-red fluorescent protein, the *mKate2* gene was cloned into the PLJM1 lentivirus vector (Addgene, Palo Alto, CA, USA). The description of lentivirus production has been described previously.[35] pMD2.G and psPAX2 were co-transfected with PLJM1-mKate2 into 293FT cells using X-tremeGENE HP DNA transfection reagent (Roche), according to manufacturer's instructions. Viral supernatants were harvested for the infection of CFPAC-1 cells. CFPAC-1 cells stably expressing far-red fluorescent protein was established by lentivirus infection and selection with puromycin using standard protocols.

Bacterial strain and culture of bacteria with CFPAC-1 cells

The luciferase gene was amplified by PCR from a PGL3 basic vector, digested with *Kpn*I and *Eco*RI, and ligated to a similarly digested pSV-SPORT plasmid to generate pSV-SPORT-luciferase. The construct was then transfected into *S. typhimurium* strain VNP20009 (ATCC, Manassas, VA, USA) by electroporation at the following conditions: 5 μF, 400 Ω, and 2400 V, using 0.2-cm cuvettes. Prior to use, the bacteria were cultured in Luria-Bertani (LB) broth from a single colony overnight, subcultured (1: 50) to mid-logarithmic phase the following day and adjusted to an appropriate concentration in phosphate-buffered saline (PBS) based on an optical density reading at 600 nm and on flat colony counting method. Bacteria and CFPAC-1cells were co-cultured as described previously.[12,36] Briefly, different strains were prepared and co-cultured with cells (infection at 100:1) at 37°C for 60 min, washed with PBS, and incubated in medium supplemented with streptomycin (20 μg/mL), penicillin(10μg/mL),and chloramphenicol (10 μg/mL) for 48 h. Cell proliferation was measured with a Cell Counting Kit-8 (CCK-8, Dojindo, Japan) at 37°C for 60 min and quantified by the absorbance at 450 nm with a plate reader.

CFPAC-1 human pancreatic subcutaneous xenograft model and bacterial application

Prior to inoculation, the tumor cells were harvested after trypsinization and passed through a cell strainer to remove cellular aggregates. The cells were then washed in culture medium, counted and diluted to 2×10^6 in 0.1 ml of culture medium. The cells were injected subcutaneously into the right flank of nude mice. The tumor size was measured with calipers. The tumor volume was calculated from the following formula: tumor volume = width^2 × length × 0.52. When tumor volumes reached the size of approximately 60–100 mm^3, the mice were randomized into 3 groups of 10 animals and intratumorally injected with *S. typhimurium* strain VNP20009 or different doses of VNP20009-luc. Twelve days after the injection, tumors and organs were aseptically removed, weighed, and homogenized in 5 volumes of ice-cold and sterile PBS. The homogenate was then plated on to LB broth media and incubated for 12 h at 37°C. The colony-forming units (cfu) per gram of tissue were determined by counting colonies.

Optical image acquisition and image formation

Fluorescence imaging and bioluminescence imaging were performed with imaging system IVIS Spectrum (Caliper, PerkinElmer) using living Images 4.3.1 software. Fluorescence of mKate2 was detected at excitation and emission wavelengths of 570 and 640 nm. For BLI analysis, the substrate D-Luciferin (CellCyto) was added at concentration of 150 μg/ml in DPBS with the culture medium removed *in vitro*. During *in vivo* imaging, animals were injected with D-luciferin at 150 mg/kg body weight, and anesthetized by 2.5% isoflurane. Peak luminescence values were recorded. After BLI analysis, fluorescence measurements were performed. The average and total radiant efficiency were measured.

Western blotting

Tumor tissues were homogenized in radioimmunoprecipitation assay (RIPA) lysis buffer (50 mmol/L Tris-HCl, 150 mmol/L NaCl, 1% Nonidet-40, 0.5% sodium deoxycholate, 1 mmol/L ethylenediamine tetraacetic acid [EDTA], 1 mmol/L phenylmethylsulfonyl fluoride [PMSF]) and centrifuged at 12,000 rpm for 30 min at 4°C. The homogenates were diluted in loading buffer, boiled at 95°C for 5 min, loaded on 12% acrylamide-sodium dodecyl sulfate (SDS) gel, and transferred to a Protran nitrocellulose membrane (Bio-Rad). The membranes were blocked with 5% dry milk in Tris-buffered saline (TBS) for 1 h at room temperature, and incubated with primary antibodies. The antibodies against caspase-3, bax, and tubulin were obtained from Cell Signaling Technology. The immunoreactivity was detected by using a standard enhanced-chemiluminescent reaction and analyzed using Image Lab 4.0 analysis sotware from Bio-Rad.

Histology and immunohistochemistry

The animals were sacrificed by an overdose of anesthesia. The tumors were removed and fixed in 4% formalin for 48 h, and then embedded in paraffin. Histological sections were prepared by standard conventional processing and stained with hematoxylin and eosin (H&E). Immunohistochemical analysis was performed on the 4-μm-thick paraffin-embedded sections using anti-Ki67 antibodies (#9027, Cell Signaling Technology). Five fields of view at a primary magnification of 200 × were selected in each tumor section. The cells were counted under a Nikon microscope, and the data are presented as means ± SEM.

Statistical analysis

Data are shown as means ± SEM. Two-tailed unpaired *Student's t* test or one-way analysis of variance test was used, followed by Tukey's test, unless otherwise stated in the figure legends. A level of $P < 0.05$ was considered statistically significant.

Disclosure of potential conflicts of interest

No potential conflicts of interest were disclosed.

References

1. Siegel RL, Miller KD, Jemal A. Cancer statistics, 2015. CA Cancer J Clin 2015; 65:5-29; PMID:25559415; http://dx.doi.org/10.3322/caac.21254

2. Feig C, Gopinathan A, Neesse A, Chan DS, Cook N, Tuveson DA. The pancreas cancer microenvironment. Clin Cancer Res 2012; 18:4266-76; PMID:22896693; http://dx.doi.org/10.1158/1078-0432.CCR-11-3114

3. Matsuo Y, Ding Q, Desaki R, Maemura K, Mataki Y, Shinchi H, Natsugoe S, Takao S. Hypoxia inducible factor-1 alpha plays a pivotal role in hepatic metastasis of pancreatic cancer: an immunohistochemical study. J Hepatobiliary Pancreat Sci 2014; 21:105-12; PMID:23798470; http://dx.doi.org/10.1002/jhbp.6

4. Zhao M, Yang M, Li XM, Jiang P, Baranov E, Li S, Xu M, Penman S, Hoffman RM. Tumor-targeting bacterial therapy with amino acid auxotrophs of GFP-expressing Salmonella typhimurium. Proc Natl Acad Sci U S A 2005; 102:755-60; PMID:15644448; http://dx.doi.org/10.1073/pnas.0408422102

5. Roberts NJ, Zhang L, Janku F, Collins A, Bai RY, Staedtke V, Rusk AW, Tung D, Miller M, Roix J, et al. Intratumoral injection of Clostridium novyi-NT spores induces antitumor responses. Sci Transl Med 2014; 6:249ra111; PMID:25122639; http://dx.doi.org/10.1126/scitranslmed.3008982

6. Maletzki C, Linnebacher M, Kreikemeyer B, Emmrich J. Pancreatic cancer regression by intratumoural injection of live Streptococcus pyogenes in a syngeneic mouse model. Gut 2008; 57:483-91; PMID:18025068; http://dx.doi.org/10.1136/gut.2007.125419

7. Forbes NS. Engineering the perfect (bacterial) cancer therapy. Nat Rev Cancer; 10:785-94; PMID:20944664; http://dx.doi.org/10.1038/nrc2934

8. Hiroshima Y, Zhang Y, Murakami T, Maawy A, Miwa S, Yamamoto M, Yano S, Sato S, Momiyama M, Mori R, et al. Efficacy of tumor-targeting Salmonella typhimurium A1-R in combination with anti-angiogenesis therapy on a pancreatic cancer patient-derived orthotopic xenograft (PDOX) and cell line mouse models. Oncotarget 2014; 5:12346-57; PMID:25402324; http://dx.doi.org/10.18632/oncotarget.2641

9. Nagakura C, Hayashi K, Zhao M, Yamauchi K, Yamamoto N, Tsuchiya H, Tomita K, Bouvet M, Hoffman RM. Efficacy of a genetically-modified Salmonella typhimurium in an orthotopic human pancreatic cancer in nude mice. Anticancer Res 2009; 29:1873-8; PMID:19528442

10. Low KB, Ittensohn M, Luo X, Zheng LM, King I, Pawelek JM, Bermudes D. Construction of VNP20009: a novel, genetically stable antibiotic-sensitive strain of tumor-targeting Salmonella for parenteral administration in humans. Method Mol Med 2004; 90:47-60; PMID:14657558

11. Thamm DH, Kurzman ID, King I, Li Z, Sznol M, Dubielzig RR, Vail DM, MacEwen EG. Systemic administration of an attenuated, tumor-targeting Salmonella typhimurium to dogs with spontaneous neoplasia: phase I evaluation. Clin Cancer Res 2005; 11:4827-34; PMID:16000580; http://dx.doi.org/10.1158/1078-0432.CCR-04-2510

12. Friedlos F, Lehouritis P, Ogilvie L, Hedley D, Davies L, Bermudes D, King I, Martin J, Marais R, Springer CJ. Attenuated Salmonella targets prodrug activating enzyme carboxypeptidase G2 to mouse melanoma and human breast and colon carcinomas for effective suicide gene therapy. Clin Cancer Res 2008; 14:4259-66; PMID:18594008; http://dx.doi.org/10.1158/1078-0432.CCR-07-4800

13. Luo X, Li Z, Lin S, Le T, Ittensohn M, Bermudes D, Runyab JD, Shen SY, Chen J, King IC, et al. Antitumor effect of VNP20009, an attenuated Salmonella, in murine tumor models. Oncol Res 2001; 12:501-8; PMID:11939414; http://dx.doi.org/10.3727/096504001108747512

14. Cheng X, Zhang X, Zhou Y, Zhang C, Hua ZC. A Salmonella Typhimurium mutant strain capable of RNAi delivery: higher tumor-targeting and lower toxicity. Cancer Biol Ther 2014; 15:1068-76; PMID:24842165; http://dx.doi.org/10.4161/cbt.29185

15. Toso JF, Gill VJ, Hwu P, Marincola FM, Restifo NP, Schwartzentruber DJ, Sherry RM, Topalian SL, Yang JC, Stock F, et al. Phase I study of the intravenous administration of attenuated Salmonella typhimurium to patients with metastatic melanoma. J Clin Oncol 2002; 20:142-52; PMID:11773163; http://dx.doi.org/10.1200/JCO.20.1.142

16. Heimann DM, Rosenberg SA. Continuous intravenous administration of live genetically modified salmonella typhimurium in patients with metastatic melanoma. J Immunother (Hagerstown, Md : 1997) 2003;

26:179-80; PMID:12616110; http://dx.doi.org/10.1097/00002371-200303000-00011

17. Piatkevich KD, Hulit J, Subach OM, Wu B, Abdulla A, Segall JE, Verkhusha VV. Monomeric red fluorescent proteins with a large Stokes shift. Proc Natl Acad Sci U S A 2009; 107:5369-74; PMID:20212155; http://dx.doi.org/10.1073/pnas.0914365107

18. Vuletic I, Liu J, Wu H, Ding Y, Lei Y, Li C, Zhu D, Ren Q, Sun H, Li J. Establishment of an mKate2-Expressing Cell Line for Non-Invasive Real-Time Breast Cancer In Vivo Imaging. Mol Imaging Biol 2015; 17:811-8; PMID:25902968; http://dx.doi.org/10.1007/s11307-015-0853-5

19. Yu YA, Shabahang S, Timiryasova TM, Zhang Q, Beltz R, Gentschev I, Goebel W, Szalay AA. Visualization of tumors and metastases in live animals with bacteria and vaccinia virus encoding light-emitting proteins. Nat Biotechnol 2004; 22:313-20; PMID:14990953; http://dx.doi.org/10.1038/nbt937

20. Contag CH, Contag PR, Mullins JI, Spilman SD, Stevenson DK, Benaron DA. Photonic detection of bacterial pathogens in living hosts. Mol Microbiol 1995; 18:593-603; PMID:8817482; http://dx.doi.org/10.1111/j.1365-2958.1995.mmi_18040593.x

21. O'Neill K, Lyons SK, Gallagher WM, Curran KM, Byrne AT. Bioluminescent imaging: a critical tool in pre-clinical oncology research. J Pathol 2010; 220:317-27; PMID:19967724; http://dx.doi.org/10.1002/path.2656

22. Shcherbo D, Murphy CS, Ermakova GV, Solovieva EA, Chepurnykh TV, Shcheglov AS, Verkhusha VV, Pletnev VZ, Hazelwood KL, Roche PM, et al. Far-red fluorescent tags for protein imaging in living tissues. Biochem J 2009; 418:567-74; PMID:19143658; http://dx.doi.org/10.1042/BJ20081949

23. Jiang SN, Park SH, Lee HJ, Zheng JH, Kim HS, Bom HS, Hong Y, Szardenings M, Shin MG, Kim SC, et al. Engineering of bacteria for the visualization of targeted delivery of a cytolytic anticancer agent. Mol Therapy 2013; 21:1985-95; PMID:23922014; http://dx.doi.org/10.1038/mt.2013.183

24. Nemunaitis J, Cunningham C, Senzer N, Kuhn J, Cramm J, Litz C, Cavagnolo R, Cahill A, Clairmont C, Sznol M. Pilot trial of genetically modified, attenuated Salmonella expressing the E. coli cytosine deaminase gene in refractory cancer patients. Cancer Gene Ther 2003; 10:737-44; PMID:14502226; http://dx.doi.org/10.1038/sj.cgt.7700634

25. Zhang Y, Zhang N, Hoffman RM, Zhao M. Comparison of the selective targeting efficacy of Salmonella typhimurium A1-R and VNP20009 on the lewis lung carcinoma in nude mice. Oncotarget 2015; 6:14625-31; PMID:25714030; http://dx.doi.org/10.18632/oncotarget.3342

26. Chen J, Wei D, Zhuang H, Qiao Y, Tang B, Zhang X, Wei J, Fang S, Chen G, Du P, et al. Proteomic screening of anaerobically regulated promoters from Salmonella and its antitumor applications. Mol Cell Proteomics 2011; 10:M111 009399; PMID:21474796; http://dx.doi.org/10.1074/mcp.M111.009399

27. Zhao M, Geller J, Ma H, Yang M, Penman S, Hoffman RM. Monotherapy with a tumor-targeting mutant of Salmonella typhimurium cures orthotopic metastatic mouse models of human prostate cancer. Proc Natl Acad Sci U S A 2007; 104:10170-4; PMID:17548809; http://dx.doi.org/10.1073/pnas.0703867104

28. Zhang Y, Miwa S, Zhang N, Hoffman RM, Zhao M. Tumor-targeting Salmonella typhimurium A1-R arrests growth of breast-cancer brain metastasis. Oncotarget 2015; 6:2615-22; PMID:25575815; http://dx.doi.org/10.18632/oncotarget.2811

29. Hiroshima Y, Zhao M, Maawy A, Zhang Y, Katz MH, Fleming JB, Uehara F, Miwa S, Yano S, Momiyama M, et al. Efficacy of Salmonella typhimurium A1-R versus chemotherapy on a pancreatic cancer patient-derived orthotopic xenograft (PDOX). J Cell Biochem 2014; 115:1254-61; PMID:24435915; http://dx.doi.org/10.1002/jcb.24769

30. Kong B, Cheng T, Wu W, Regel I, Raulefs S, Friess H, Erkan M, Esposito I, Kleeff J, Michalski CW. Hypoxia-induced endoplasmic reticulum stress characterizes a necrotic phenotype of pancreatic cancer. Oncotarget 2015; 6:32154-60; PMID:26452217; http://dx.doi.org/10.18632/oncotarget.5168

31. Matsuoka H, Shibamoto Y, Kubota T, Tsujitani M, Majima T. In vivo efficacy and pharmacokinetics of a new hypoxic cell radiosensitizer doranidazole in SUIT-2 human pancreatic cancer xenografted in mouse pancreas. Oncol Rep 2000; 7:23-6; PMID:10601585; http://dx.doi.org/10.3892/or.7.1.23

32. Yu B, Yang M, Shi L, Yao Y, Jiang Q, Li X, Tang LH, Zheng BJ, Yuen KY, Smith DK, et al. Explicit hypoxia targeting with tumor suppression by creating an "obligate" anaerobic Salmonella Typhimurium strain. Sci Rep 2012; 2:436; PMID:22666539; http://dx.doi.org/10.1038/srep00436

33. Avogadri F, Martinoli C, Petrovska L, Chiodoni C, Transidico P, Bronte V, Longhi R, Colombo MP, Dougan G, Rescigno M. Cancer immunotherapy based on killing of Salmonella-infected tumor cells. Cancer research 2005; 65:3920-7; PMID:15867392; http://dx.doi.org/10.1158/0008-5472.CAN-04-3002

34. Schoumacher RA, Ram J, Iannuzzi MC, Bradbury NA, Wallace RW, Hon CT, Kelly DR, Schmid SM, Gelder FB, Rado TA. A cystic fibrosis pancreatic adenocarcinoma cell line. Proc Natl Acad Sci U S A 1990; 87:4012-6; PMID:1692630; http://dx.doi.org/10.1073/pnas.87.10.4012

35. Pan J, Cheng L, Bi X, Zhang X, Liu S, Bai X, Li F, Zhao AZ. Elevation of omega-3 Polyunsaturated Fatty Acids Attenuates PTEN-deficiency Induced Endometrial Cancer Development through Regulation of COX-2 and PGE2 Production. Sci Rep 2015; 5:14958; PMID:26468779; http://dx.doi.org/10.1038/srep14958

36. Eisenstark A, Kazmierczak RA, Dino A, Khreis R, Newman D, Schatten H. Development of Salmonella strains as cancer therapy agents and testing in tumor cell lines. Methods Mol Biol (Clifton, NJ) 2007; 394:323-54; PMID:18363243; http://dx.doi.org/10.1007/978-1-59745-512-1_16